Journal of the Korean Vacuum Society
Vol. 2, No. 1, March 1993, pp. 58-64

〈연구논문〉

A Model for Atomic Transport at Low Temperature Ion Mixing

K.H. Chae, J.H. Song, S.M. Jung, H.G. Jang, J.H. Joo, S.T. Kang
B.S. Choi[1], S.O. Kim[2] and C.N. Whang

Department of Physics, Yonsei University, Seoul 120-749, Korea
[1]Department of Physics, Jeonju University, Jeonju 560-759, Korea
[2]Department of Physics, Seonam University, Namwon 590-170, Korea
(Received December 22, 1992)

저온에서 이온선 혼합시 야기되는 원자이동에 대한 모형

채근화 · 송종한 · 정성문 · 장흥규 · 주장헌
강석태 · 최범식[1] · 김상옥[2] · 황정남

연세대학교 물리학과, [1]전주대학교 물리학과
[2]서남대학교 물리학과
(1992년 12월 22일 접수)

Abstract—A simple model is presented to describe quantitative the isotropic and anisotropic atomic transport in thermal spike induced ion mixing. The ratio of atomic transport depends on the activation energies of constituents for the impurity diffusion. The model predicts fairly satisfactory the trend of experimental observations for the bilayer systems which have near zero heats of mixing and relatively high spike activation energies. The systems which have large difference in activation energies of constituents for the impurity diffusion show the anisotropic atomic transport, while the systems having similar activation energies for the impurity diffusion reveal the isotropic atomic transport.

요 약—이온선혼합의 열충격으로 야기되는 등방적 또는 이방적 원자이동을 정량적으로 묘사하기 위한 모형을 제시하였다. 불순물 확산에서 원자들의 이동비는 구성원자들의 활성화에너지에 의존한다. 이 모형은 0에 가까운 혼합열과 비교적 높은 활성화에너지를 가진 이중층들의 실험결과들을 만족스럽게 예견한다. 불순물 확산에서 구성원자들의 활성화에너지가 크게 차이가 나는 계들은 이방적 원자이동을 보여주는 반면, 비슷한 활성화에너지를 가지는 계들은 등방적 원자이동을 나타낸다.

1. Introduction

Recent rapid progress in using ion beam techniques has been attracting a great attention in view of surface and interface modification of materials. This modification can be achieved by introducing suitable impurities using ion beam mixing technique, which has advantages to produce some metastable compositions and structures not existing in the equilibrium state. The atomic mixing due to ion bombardment at low temperature was proposed to arise mainly from collisional effect[1] and/or thermal spike effect[2]. However the basic mechanisms of ion beam mixing is not fully understood because of complicity of mixing phenomenon. Especially, it is not well known about the atomic

transport of consituents across the interface in bilayer or multilayer system.

Recently, Auner *et al*[3-5] have presented experimental results for the isotropic or anisotropic atomic transport in ion beam mixing at low temperature, and developed a qualitative model to understand the experimental observations, which is related with the difference of the cohesive energy of each side in a bilayer, and the fractal geometry for the thermal spike formation; that is, a preferential atomic transport from the high cohesive energy side to the low cohesive energy side is arisen due to the thermal spike contribution to ion mixing, an isotropic atomic transport in bilayers consisting of similar and low cohesive energy is also due to the thermal spike effect because of its high probability of spike formation, and a preferential inward atomic transport in bilayers consisting of elements of similar and high cohesive energy is result of the cascade collisional contribution. However their model can predict only qualitatively the isotropic or the anisotropic atomic transport. It cannot determine the absolute amount of atomic transport or the ratio of atomic transport across the interface in ion beam mixing at low temperature.

In this study, we present an experimental result for the isotropic atomic transport in Pd/Co bilayer due to thermal spike induced ion mixing, and develop a model to predict the absolute ratio of atomic transport of constituents in bilayer systems, which is based on the Vineyard's thermal spike model[6] and the impurity diffusion in solid by a vacancy mechanism[7].

2. Experimental Procedures

The amounts of atomic transport flux were measured from the movement of a marker embedded at the interface between the Pd/Co bilayer. A thin layer of Au(10 Å) was used as a marker for Pd/Co bilayer study,because it has[8] zero heat of mixing with Pd and a positive heat of mixing(+11 kJ/g. at.) with Co. Pd/Co system was chosen due to their larger mass difference, near zero heat of mixing[8] (−2 kJ/g. at.), and their similar and low cohesive energies[9] (3.89 eV for Pd and 4.39 eV for Co). This structure (Pd/Au/Co) is well suited for studying the isotropic atomic transport in absence of thermo-chemical driving force associated with the heat of mixing.

Pd (300 Å, top layer)/Au (10 Å, marker)/Co (1000 Å, bottom layer) samples were deposited on single crystal Si substrates by sequential electron beam evaporation, at a base pressure of less than 2×10^{-7} Torr and a pressure of 8×10^{-7} Torr during deposition. The depth of the marker was chosen to match with the mean projected range of 80 keV Ar^+ ions in the Pd layer. Ion beam mixing was carried out with 80 keV Ar^+ ions at 90 K in order to avoid radiation enhanced diffusion; the critical temperature[10] for radiation enhanced diffusion in this system would be about 400 K. The ion dose ranged between 1×10^{15} and 2×10^{16} Ar^+/cm^2 at a typical flux of 1.5 $\mu A/cm^2$. The amounts of intermixing of Pd and Co atoms and the movement of Au marker were evaluated with Rutherford backscattering spectroscopy(RBS). For RBS observation, the target was tilted to an angle of 60° from the incident 2.425 MeV He^+ beam, and the energy of the backscattered He^+ was analyzed at a laboratory scattering angle of 170° with a detector of 14 keV nominal energy resolution.

The composition profiles of Pd and Co atoms and the amount of atomic transport were determined using the computer simulation for RBS spectra[11]. The atomic transport across the marker layer from the top layer (Pd) to the bottom layer (Co), J_A, and vice versa, J_B, were evaluated using computer simulation with considering the sputtering effects.

3. Results and Discussions

3.1. Experimental Results for Pd/Co Bilayer

Fig. 1 shows the RBS spectra of Pd and Au layer for the as-deposited and 1.2×10^{16} Ar^+/cm^2 irradiated samples. After ion bombardment at 90 K, the portion of low energy edge of Pd signal shifts to lower energy, and the shape of the marker signal becomes broader. The broadening of the marker signal and the shift of the low-energy edge of Pd signal are enhanced progressively with inceasing ion dose, which demonstrate the atomic transport

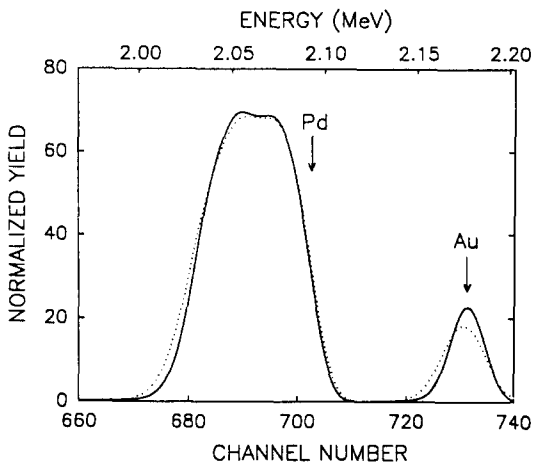

Fig. 1. Rutherford backscattering spectra of the Pd and Au layer for the as-deposited (—) and 1.2 $\times 10^{16}$ Ar^+/cm^2 irradiated (···) Pd/Au/Co system.

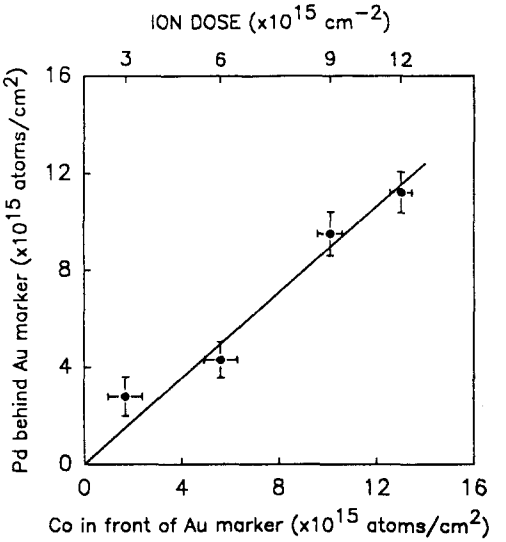

Fig. 2. Movements of Pd and Co atoms across the Au marker at various ion doses.

has occurred by ion bombardment. But the marker position remains almost stationary. The shift of marker position is opposite to the direction of the atomic transport. Thus the stationary movement of marker in Fig. 1 indicates that the atomic mixing of Pd and that of Co across the marker layer is nearly same amount, or the isotropic atomic transport has occurred in Pd/Co system during ion mixing at 90 K.

The atomic transport across the marker layer were determined at various ion doses by fitting the computer simulated curves to the experimentally observed RBS specta. Fig. 2 shows the atomic transport of Pd and Co at various ion doses. The ratio of the atomic transport of Pd to that of Co, J_A/J_B, is found to 0.86± 0.08. Thus the Pd/Co system shows nearly isotropic atomic transport by ion mixing at low temperature.

3.2. Model for Atomic Transport in Ion Mixing at Low Temperature

In order to interpret our experimental results and develop a model to predict the value of J_A/J_B, we introduce the Vineyard's thermal spike model [6] and normal impurity diffusion in solid[7]. Vineyard's model assumes that the atomic jumping rate in the thermal spike region is given by

$$\eta_r = A \exp(-Q/kT) \quad (1)$$

where A and Q are the temperature independent preexponential factor and the activation energy for the thermal spike, respectively, and T is the spike temperature evolved in space and time according to the laws of classical heat conduction. The total number of atomic jumps in one spike per unit length of spike can be obtained by integrating the eq. (1) over space and time,

$$\eta = C_1 \left[\frac{F_d}{Q} \right]^n \quad (2)$$

where C_1 is constant associated with the thermal conductivity for lattice heat conduction and the specific heat of the target, F_d is the energy deposited per unit ion path length at the interface, and n is the power factor. The value of n is 2 for the cylindrical thermal spike, and 5/3 for the spherical thermal spike. The total number of jumps per target atoms in the material after being irradiated with ion dose ϕ is $\eta\phi/\rho$, where ρ is the average atomic density of target materials. The effective diffusion coefficient can be expressed[12] as $D=(\eta\phi/\rho t)\, r^2_c$, where t is the irradiation time and r_c is the characteristic atomic jumping distance. r_c can be assumed to be related to ρ, $r_c = s\, \rho^{-1/3}$. And the atomic

transport (atoms/cm^2) across the interface is given [13] by $J=Dt\rho\ \partial f(x)/\partial x$, where f(x) is the stoichiometric fraction of atom at a depth of x. Thus the atomic transport becomes

$$J=C_2\left(\frac{F_d}{Q}\right)^n \frac{\phi}{\rho^{2/3}} \frac{\partial}{\partial x} f(x) \tag{3}$$

where C_2 is a constant.

In eq. (3), the atomic transport across the interface is related to the thermal spike activation parameter[6] $\chi=F_d/Q$. When the activation energies for the thermal spike of constituents in bilayer are different, the degree of atomic transport should correlate with the difference in χ of each side in the bilayer as like as the normal impurity diffusion in solid. Moreover Kim *et al*[14] observed a correlation between ion mixing at low temperature and the normal impurity diffusion. Thus the thermally activated diffusional process in the thermal spike region could be assumed to be related with the normal impurity diffusion in solid.

For a given pair of impurity and matrix, the activation energy for an impurity atom A to diffuse into a matrix atom B, $Q_{A(B)}^*$ can be expressed as [15]

$$Q^*_{A(B)}=Q_B+\Delta Q \tag{4}$$

where Q_B is the activation energy for the self diffusion of the matrix element, and ΔQ is the difference between $Q_{A(B)}^*$ and Q_B. The activation energy for self diffusion is[15]

$$Q_B=E^B_{vf}+E^B_{vm} \tag{5}$$

where E^B_{vf} and E^B_{vm} are vacancy formation and vacancy migration energies of the matrix element, respectively. The difference of the activation energy, ΔQ, can be expressed as[7]

$$\Delta Q=\Delta E_f+\Delta E_m-C \tag{6}$$

where ΔE_f and ΔE_m are the difference of vacancy migration and formation energies, and C is the correlation correction term, which is usually small[15] compared with the first two terms in eq. (6). Neumann and Hirschwald[7] proposed a model for the impurity diffusion, and derived a relation between ΔE_m and melting points of impurity and matrix elements,

$$\Delta E=\frac{E^B_v m}{2}\left(\frac{T^A_m}{T^B_m}-1\right) \tag{7}$$

where T^A_m and T^B_m are melting points of the impurity and matrix elements, respectively. And also they derived a relation between ΔE_f and ΔE_m,

$$\Delta E_f=0.17\ \Delta E_m \tag{8}$$

Using the relation[15] between the E^B_{vm} and Q_B ($E^B_{vm}=0.47\ Q_B$), eq. (7), and (8), eq. (6) becomes, neglecting the correlation correction term,

$$\Delta E=0.275\ Q_B\left(\frac{T^A_m}{T^B_m}-1\right) \tag{9}$$

The melting point of material has been derived[16] to be scaled with its cohesive energy, $T_m=0.032\ E_{coh}/k$. Thus eq. (9) becomes

$$\Delta E=0.275\ Q_B\left(\frac{E^A_{coh}}{E^B_{coh}}-1\right) \tag{9}$$

where E^A_{coh} and E^B_{coh} are the cohesive energies of the impurity and the matrix element, respectively. Furthermore, for self diffusion in metals, there is an established correlation[17, 18] between E^B_{vf}, Q_B and E^B_{coh}, $E^B_{vf}=0.55\ Q_B=0.29\ E^B_{coh}$, that is,

$$Q_B=0.53\ E^B_{coh} \tag{11}$$

Combining eq. (4), (10) and (11), the activation energy for the impurity diffusion becomes

$$Q^*_{A(B)}=0.38\ E^B_{coh}+0.15\ E^A_{coh} \tag{12}$$

In a bilayer system composed of A and B atoms, the activation energy $Q_{A(B)}^*$ for A atoms to diffuse into the matrix of B atoms should be different from $Q_{B(A)}^*$, when the values of E^A_{coh} and the E^B_{coh} are different. Ma[12] has shown that there exists a scaling relationship between the activation energy for the thermal spike induced diffusion and that for vacancy self diffusion, and recent molecular dynamic computer simulation results[19] show that melting have occurred in a thermal spike. Therefore, it is reasonable to assume a scaling relationship between the activation energy in a thermal spike, Q, and that for the normal impurity diffusion

in solid, $Q_{A(B)}^*$. The value of F_d in eq. (1) varies smoothly on each side of the interface when the mean projected range of ion and its standard deviation ($R_p+\Delta R_p$) spread in a larger region around the interface[20]. Thus we assume that the value of F_d is constant at the interface. When we assume that the values of F_d and ρ are constant, the activation energy for the thermal spike scales with the activation energy for the impurity diffusion, and the concentration gradients of constituents in a bilayer, $\partial f(x)/\partial x$, are approximately equal on each side of the bilayer interface, the ratio of the atomic transport of A and B atoms across the interface in the thermal spike region can be expressed approximately as, from eq. (3),

$$\frac{J_A}{J_B}=\left(\frac{Q^*_{B(A)}}{Q^*_{A(B)}}\right)^n \tag{13}$$

From eq. (13), one can easily recognize that the ratio of atomic transport depends on the activation energies for the impurity diffusion, and the system having large difference between $Q_{A(B)}^*$ and $Q_{B(A)}^*$ shows an anisotropic atomic transport, while the system which has similar Q^* values of constituents reveals an isotropic atomic transport.

3.3. Comparison between the Experimental and Calculated Results

The above model is compared with experimentally determined ratio of atomic transport in low temperature ion mixed bilayer system. The thermal spike shape can be identified[21] by the value of χ; that is, the cascade collisional mixing region has a low value of χ (<22 Å^{-1}), the spherical thermal spike region has a relatively high vlaue of χ (22 Å$^{-1}\leq\chi<75$ Å^{-1}), and the cylindrical thermal spike region has a extremely high value of χ (≥ 75 Å^{-1}). When we define $\chi\approx F_d/Q^*$, the value of χ for the Pd/Co system is found to be roughly 45 Å^{-1}, since the valus of $Q_{Pd(Co)}^*$, $Q_{Co(Pd)}^*$ and F_d are 2.25 eV, 2.14 eV and $\sim$100 eV/Å, respectively, where the value of F_d at the interface of the Pd/Co system was obtained using dynamic Monte-Carlo simulation program[22] containing not only cascade collision but also sputtering effects. Therefore our experimental result for the Pd/Co system might be arisen due to the spherical thermal spike induced diffusion. Using the values of $Q_{Pd(Co)}^*$, $Q_{Co(Pd)}^*$, $\rho_{Pd}=6.80\times10^{22}$ cm^{-3}, $\rho_{Co}=8.97\times10^{22}$ cm^{-3} and $n=5/3$, we found that the value of J_A/J_B is 0.92 from eq. (13). These value is in good agreement with the experimental results of $J_A/J_B=0.86\pm0.08$. This isotropic atomic transport in the Pd/Co system is an expected result, since the constituents (Pd and Co) of this system have similar activation energies for the impurity diffusion.

In order to clarify the validity of the present model, we compare the Auner *et al*'s experimental results[3] with the predicted values from the present model. Auner *et al*[3] introduced a dimensionless atomic transport defined by $J_i^*=J_i/\rho_i^{2/3}$ (i=A or B), then the ratio of dimensionless atomic transport becomes from eq. (13) as,

$$\frac{J^*_A}{J^*_B}=\left(\frac{Q^*_{B(A)}}{Q^*_{A(B)}}\right)^n\left(\frac{\rho_B}{\rho_A}\right)^{2/3} \tag{14}$$

In table 1, we tabulate the measured and calculated values of J_A^*/J_B^* for various systems, along with some parameters required for eq. (14). Fig. 3 shows the comparison between the measured and calculated values of J_A^*/J_B^*. We use the value of $n=2$ for the systems in Ref. [3], because they have extremely high values of χ (>100 Å^{-1}). The linear line in Fig. 3 indicates calculated values using eq. (14). It can be seen that the agreement between the experimental results and the calculated ones are fairly satisfactory except for the W/Pd case. We suppose that the disagreement in W/Pd system might be arisen due to its high chemical driving force because of its relatively high negative value of heat of mixing (-11 kJ/g. at)[8] compared to other systems in Fig. 3.

The present model can be used to calculate the transport of marker element in the consitituents of the bilayer. The shift of mean position of the marker layer is related[23] with the heat of mixing of the marker element in the constituents of bilayer. When the heat of mixing of marker element in the constituents is near zero as like as this study or Auner[3] *et al*'s study, the shift of mean position of the marker layer can be described only by the unbalanced transport of the constituents across the

Table 1. System geometries, cohesive energies (E_{coh})[a], atomic densities (ρ)[b], activation energies or impurity diffusion ($Q_{A(B)}^*$)[c], the experimental and the calculated values of the ratio of dimensionless fluxes ($(J_A^*/J_B^*)_{exp}$[d], $(J_A^*/J_B^*)_{cal}$[e]).

System configuration (A/B)	E_{coh}^A (eV/atom)	E_{coh}^B (eV/atom)	$Q_{A(B)}^*$ (eV/atom)	ρ_A ($\times 10^{22}$/cm^3)	ρ_B ($\times 10^{22}$/cm^3)	$(J_A^*/J_B^*)_{cal}$	$(J_A^*/J_B^*)_{exp}$
W/Pd	8.90	3.89	2.81	6.30	6.80	1.18	2.09
Pd/W	3.89	8.90	3.97	6.80	6.30	0.73	0.48
Nb/Cu	7.57	3.49	2.46	5.56	8.45	2.78	2.53
Cu/Nb	3.49	7.57	3.41	8.45	5.56	0.48	0.39
V/Ag	5.31	2.95	1.92	7.22	5.85	1.54	1.43
Ag/V	2.95	5.31	2.46	5.85	7.22	0.50	0.70
Ni/Pd	4.30	3.89	2.12	5.14	6.80	1.18	1.33
Pd/Ni	3.89	4.30	2.22	6.80	5.14	0.96	0.88
Pd/Co	3.89	4.39	2.25	6.80	8.87	1.03[f]	1.11[g]

[a] from Ref. [9].
[b] W. K. Chu, J. W. Mayer and M. -A. Nicolet. *Backscattering Spectrometry* (Academic Press, New York, 1978) p. 344.
[c] calculated using eq. (12).
[d] from Ref.[3]
[e] calculated using eq. (14).
[f] this study.
[g] n=5/3 is used for the eq. (14).

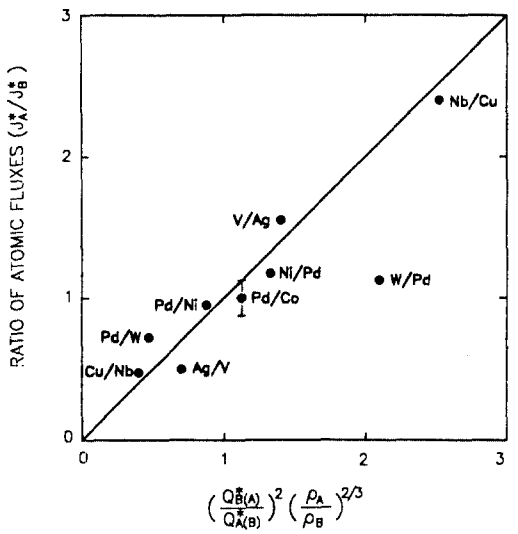

Fig. 3. Comparision between the measured and calculated ratio of atomic transport in bilayered systems. The line is the calculated values using eq. (14) (n=2 for the systems from Ref. [13] and n=5/3 for the Pd/Co system).

interface. However, even in this case, the mean spread of Gaussian profile for the marker element is related with the activation energy, Q, in eq. (1). Ma[12] described the Gaussian spread (Ω^2) of marker elements in noble metal matrices using similar relation with eq. (12); that is, the ratio of the spread of Au marker in Pd and Co can be described by eq. (13). The value of $\Omega^2_{Au(Pd)}/\Omega^2_{Au(Co)}$ is found to be 1.16 using n=5/3, which mean that the shape of Au marker distribution is a symmetric Gaussian profile as shown in Fig. 1. We estimate also the ratio of spread in Gaussian profile of Ta marker layer for the Cu/Ta/Nb system in the Ref. [3]. The value of $\Omega^2_{Ta(Cu)}/\Omega^2_{Ta(Nb)}$ is found to be 2.59 using n=2 for the eq. (13). This means that the shape of Ta marker distribution reveals an asymmetric Gaussian profiles having a wider spread in Cu side than in Nb side, which is in good agreement with the experimental result[5]. Thus the present model can be used phenomenologically to determine the shape of Gaussian distribution of marker layer in the thermal spike induced ion mixing.

4. Conclusions

Thermal spike mechanism dominates at low

temperature ion beam mixing in bilayer systems which have near zero heats of mixing and relatively high spike activation parameters. And the ratio of atomic transport of constituents due to thermal spike is related with the effective energies of constituents for the impurity diffusion. For instance, the Pd/Co bilayer system shows an isotropic atomic transport because of its relatively high spike activation parameter and similar activation energies of its constituents for the impurity diffusion. A model to describe the ratio of atomic transport in thermal spike induced diffusion, which is based on the Vineyard's thermal spike model and the normal impurity diffusion, correctly predicts the trend in experimental observation and agree fairly well quantitatively with the measured ratio of atomic transport in bilayer systems which have nearly zero heat of mixing and relatively high spike activation parameter.

Acknowledgment

This work was supported in part by the Korea Science and Engineering Foundation and Ministry of Education.

References

1. P. Sigmund and A. Gras-Marti, Nucl. Instrum. Methods. **182/183**, 25 (1981).
2. W. L. Johnson, Y.-T. Cheng, M. van Rossum and M.-A. Nicolet, *Nucl. Instrum. Methods* **B5/8**, 657 (1985).
3. Y.-T. Cheng, G. W. Auner, M. H. Alkaisi, K. R. Padmanabahn and M. M. Karmarkar, *Nucl. Instrum. Methods* **B59/60**, 509 (1991).
4. G. W. Auner, Y.-T. Cheng, M. H. Alkaisi and K. R. Padmanabahn, *Appl. Phys. Lett.* **58**, 586 (1991).
5. G. W. Auner, Y.-T. Cheng, M. H. Alkaisi, M. M. Karmarkar and K. R. Padmanabahn, *Nucl. Instrum. Methods* **B59/60**, 504 (1991).
6. G. H. Vineyard, Radiat. Eff. **19**, 245 (1976).
7. G. Neumann and W. Hirschwald, *Phys. Stat. Sol.* (b) **55**, 99 (1973).
8. A. R. Miedema, *Phil. Techn. Rev.* **36**, 217 (1976).
9. C. Kittel *Introduction to Solid State Physics,* 5th ed. (Wiley, NY, 1976) p. 74.
10. Y.-T. Cheng, X.-A. Zhao, T. Banwell, T. W. Workman, M.-A. Nicolet and W. L. Johnson, *J. Appl. Phys.* **60**, 2615 (1986).
11. L. R. Doolitle, *Nucl. Instrum. Methods.* **B15**, 227 (1986).
12. E. Ma, *Nucl. Instrum. Methods* **B58**, 194 (1991).
13. P. K. Haff and Z. E. Switowski, *J. Appl. Phys.* **48**, 3383 (1977).
14. S. J. Kim, M.-A. Nicolet, R. S. Averback and D. Peak, *Phys. Rev.* **B37**, 38 (1988).
15. A. D. Le Claire, *J. Nucl. Matter,* **69/70**, 70 (1978).
16. F. Guinea, J. H. Rose, J. R. Smith and J. Ferrante, *Appl. Phys. Lett.* **44**, 53 (1984).
17. R. O. Simmons and R. W. Balluffi, *Phys. Rev.* **129**, 1533 (1963).
18. M. Doyama and J. S. Koehler, *Acta Metall.* **24**, 871 (1976).
19. T. D. de la Ribia, R. S. Averback, R. Benedek and W. E. King, *Phys. Rev. Lett.* **59**, 1930 (1987).
20. M. A. S. Vascincellos, J. A. T. Berges, P. L. Grande, S. R. Teixeira, W. H. Schreiner, I. J.R. Baumvol and C. Scherer, *Phys. Stat. Sol(a)* **129**, 453 (1992).
21. G. S. Chen, D. Farkas and M. Rangaswamy, *Mat. Res. Soc. Symp. Proc.* **128**, 195 (1989).
22. J. H. Kim, H. J. Kang, K. H. Chae, J. H. Song, J. J. Woo, C. N. Whang, H. K. Kim and D. W. Moon, *Nucl. Instrum. Methods* **B71**, 271 (1992).
23. F. Ding, R. S. Averback and H. Hahn, *J. Appl. Phys.* **64**, 1785 (1988).